www.coast.oaustech.edu.ng
COAST
JOURNAL OF THE SCHOOL OF SCIENCE
Volume 3, Issue 2. November, 2021 ISSN: 2714-3716
Coast, J. Sch. Sci. 3 (2): 682- 697

SELECTIVE ADSORPTION OF Fe (II) OVER Zn (II) FROM PHARMACEUTICAL WASTEWATER

[1*]Aderibigbe, F. A., [2]Saka, H. B., [3, 4]Amosa, M. K., [1]Idris, M. O., [1]Bello, T. B., [1]Olufowora, F. O., [1]Adebayo, R. O. and [1]Suleiman, S.

[1] Department of Chemical Engineering, University of Ilorin, Ilorin, Nigeria
[2]Quality Control Department, Segmax Oil Nigeria Limited, Kere-Aje, Ogbondoroko, Kwara State, Nigeria
[3]Waste Management Unit, HSE Division, Department of Petroleum Resources, 7, Sylvester Ugoh Crescent, Jabi, Abuja-FCT, Nigeria.
[4]National Improved Oil Recovery Centre, NOGEC Complex, 7, Kofo Abayomi Street, Victoria Island, Lagos, Nigeria.
*Corresponding Author's Email: aderibigbe.fa@unilorin.edu.ng

Abstract
This work focused on the utilization of termite mound clay and activated carbon prepared from groundnuts pod for the selective removal of Fe (II) over Zn (II) from Pharmaceutical Wastewater. The initial concentration of Fe (II) [0.46 mg/l] and Zn (II) [0.10mg/l] in the pharmaceutical wastewater were determined using Atomic Absorption Spectrophotometer (AAS). Scanning Electron Microscopy (SEM) technique, Fourier transforms infrared (FT-IR) spectroscopy, X-Ray fluorescence (XRF) and X-ray diffraction (XRD) were conducted to investigate the adsorbent features. A preliminary experiment was carried out to determine the suitable adsorbent for optimization studies. Optimization study using Box-Behnken experimental design in Response Surface Methodology were employed. The coded levels selected includes adsorbent loading between 0.05- 0.15 g, temperatures 25 - 45 °C and time 30 - 90 mins. At Optimal condition, 6.6 pH value, the temperature of 25 °C, contact time of 90 mins and adsorbent dosage of 0.1 g, the Fe (II) in the Pharmaceutical Wastewater was removed by 95.72 %. The Langmuir adsorption isotherm model was found to have R^2 of 0.9997. The adsorption capacity of the adsorbent was found to be 0.44 mg/g. Adsorption of Fe (II) onto groundnut pod activated carbon and termite mound clay was best described by the pseudo first order kinetic model (R^2 = 1.000). The termite mound clay and the activated carbonized groundnuts pod shows an effective adsorption towards the removal of the targeted pollutant from the pharmaceutical wastewater.
Keywords: adsorption, Box Behnken design, groundnuts pod, pharmaceutical wastewater, termite mound.

Introduction

Water pollution is one of the most serious environmental problems being faced by modern society. One important water pollutant are heavy metals. Heavy metals are known for their non-degradability and toxicity (Ali et al., 2014). Some metal ions are cumulative poisons capable of being

assimilated and stored in the tissues of organisms, causing noticeable adverse physiological effects —(Gupta and Ali, 2004).

Although there are many sources of heavy metals, specifically industrial sectors are at present those which mostly contribute to the release of heavy metals to the environment. Moreover, mining wastes and acid mine drainage contribute significant quantities of dissolved copper to effluent streams (Larsson, 2018). Other sources are pharmaceuticals, fertilizer manufacturing, petroleum refining, paints and pigments, steelworks, foundries, electroplating and electrical equipment and brass (Stylianou et al., 2007). However, with the development of the pharmaceutical industry, environmental pollution is becoming more hazardous.

Due to the variety of the pharmaceutical industry products, the wastewater generates high-concentrated antibiotic wastewater, which contains high metals concentration from drugs, high sulfate concentration, complicated composition, and biological toxicity. Traditional treatment methods of pharmaceutical wastewater are expensive and difficult to satisfy the demand. Therefore, advanced treatment of pharmaceutical wastewater is essential(Chen et al., 2018).

Several techniques like chemical precipitation, evaporation, solvent extraction, ion exchange, electrochemical treatment, and membrane filtration technologies have been used to remove these hazardous pollutants from wastewater ——(Gupta et al., 2009). However, these techniques are not suitable to use in the removal of low metal concentrations which cause damage to the ecosystem (Mohamed, 2013). Therefore, the adsorption process is a suitable technique for inorganic and organic pollutants removal from wastewater, because of the significant advantages such as cost-effectiveness, availability of required resources, ease of operation and efficiency (Trivedi and Mandavgane 2016).

Researchers have reported the use of different adsorbents which include biomass materials, zeolites, silica gel, activated carbon and ash for wastewater treatment (Gisi *et al.*, 2016). Attention has been drawn to natural materials capable of removing pollutants from contaminated wastewaters. Therefore, the exploration of readily available natural adsorbents that effectively treat wastewater with or without the initial treatment processes is pertinent.

Extensive literature survey has shown the use of termite mound clay and groundnut pod as natural adsorbent for the removal of heavy metals such as chromium, arsenic and excess fluoride but not much literature have reported that simultaneous use of both termite mound and groundnuts pod for the treatment of pharmaceutical wastewater Trivedi et al., 2016)(Habeeb et al.,2014; . Their main advantage over other low-cost adsorbents is that they are readily available and affordable. Therefore, this study attempts to employ the simultaneous use of termite mound clay and groundnuts pod for the removal of iron and zinc from the pharmaceutical wastewater in Ilorin Urban Center, Kwara State, Nigeria.

Materials and Methods

The materials required for this research includes H_3PO_4 (99.9%), KOH (99.98%), termite mound clay and groundnuts pod. The termite mound was obtained from the metropolis of the University of Ilorin, Ilorin, Kwara State while the groundnuts pod was obtained from *Oja Tun-Tun* Market in Ilorin. Industrial wastewater was obtained from a Pharmaceutical Industry in Ilorin, Ilorin, Kwara State. The H_3PO_4 (99.9%) and KOH (99.98%) were analytical grade products from

Sigma Aldrich, representative in Nigeria.

Carbonization and Chemical Activation of Groundnuts Pod

The groundnuts pod (120 g) was washed gently with distilled water to remove mud and other impurities, sun-dried for 24 h, beneficiated, sieved and then oven-dried at 50^{0}C for 12 h until a constant weight was achieved. To carry out the chemical activation, phosphoric acid (H_3PO_4) was impregnated into the dried groundnuts pod in the ratio of 1:15 w/v (that is 60 g of groundnuts pod to 750 ml of 1.0 M H_3PO_4). The mixed sample was thoroughly stirred with a magnetic stirrer for 4 h until a paste was formed. The stirred sample was left for 24 h. Thereafter, the paste was oven-dried at 80 °C for 24 h. The sample was divided into three parts of 20g each, transferred into crucibles and then carbonized in the muffle furnace (Model No: VE-40, Vimal Enterprise) at 350, 450 and 500 °C respectively for 2 h (Sinica, 2012). The activated sample was then cooled at room temperature and neutralized with 1 M KOH. It was then dried in an oven at 105 °C for 3 h. Finally, the chemically activated and carbonized groundnuts pod (CCG) was sieved to particle size of 0.420 mm and labeled A_1, A_2 and A_3 calcined at 350 450 and 500 °C respectively. The labeled samples were stored in the desiccator before use (Cabriga *et al.,* 2021; Ali *et al.,* 2006).

Preparation of Termite Mound

The harvested termite mound in lump form was manually pulverized using mortar and pestle and then was dispersed in distilled water and wet- sieved. Thereafter, the fine termite mound powder was dried in an oven at 105 °C for 4 h to eliminate moisture content and then sieved through a sieve mesh of 0.3 mm to obtain a particle size less than 0.354 mm. It was thermally heated at separate temperatures; 700, 800 and 900 °C respectively for 2 h in a preheated Muffle Furnace (Model No: VE-40, Vimal Enterprise) and then labeled B_1, B_2 and B_3 at calcination temperature 700, 800 and 900 °C respectively (Fufa, 2016). The labeled samples were stored in airtight plastic bottles before adsorption experiments.

Adsorbent Ratios

The prepared samples (A_1, A_2 and A_3; B_1, B_2 and B_3) were mixed in different ratios of (1:1), (1:2) and (2:1) as illustrated in Table 1. Initially, the adsorbent dosages of 0.067, 0.05 and 0.033 g were used in a preliminary experiment to determine the best mixing ratio for the optimization process.

Table 1. Mixing Ratios of A_1, A_2, A_3, B_1, B_2 and B_3

A_1: B_1	A_2: B_2	A_3: B_3	A_1: B_2	A_1: B_3	A_2: B_1	A_2: B_3	A_3: B_1	A_3: B_2
1:1(M1)	1:1(M7)	1:1(M4)	1:1(M10)	1:1(M13)	1:1(M16)	1:1(M19)	1:1(M22)	1:1(M25)
1:2(M2)	1:2(M8)	1:2(M5)	1:2(M11)	1:2(M14)	1:2(M17)	1:2(M20)	1:2(M23)	1:2(M26)
2:1(M3)	2:1(M9)	2:1(M6)	2:1(M12)	2:1(M15)	2:1(M18)	2:1(M21)	2:1(M24)	2:1(M27)

Adsorption Experiments

The batch adsorption process was carried out based on 100 ml of the wastewater containing Fe (II) and Zn (II) ions. A typical sample of adsorbent (0.067g) was charged into each conical flask. Thereafter, the set of flasks containing the wastewater and adsorbent were placed in a thermostatic water bath shaker operating at a constant

temperature of 35 °C and agitation speed of 120 rpm until the adsorption process attained an equilibrium contact time of 60 mins. This process was repeated for the 27 adsorbents at different adsorbent dosages of 0.05 and 0.033 g to make a total of 81 applications in the preliminary adsorption and only the adsorbent loading of 0.05 with the best results were reported out of 81 experimental runs.

The sample A_2B_1 at ratio 2:1 and absorbent loading of 0.05 with the best removal efficiency was used for the optimization process in Box-Behnken design under the Response Surface Methodology (RSM) in Design Expert 10.0.1. For optimization purposes, the adsorbent loadings 0.05, 0.1 and 0.15 g, temperatures of 25, 35 and 45 °C and time of 30, 60 and 90 mins and fixed agitation of 120 rpm were utilized. The removal efficiency of Fe(II) and Zn(II) ions was thus calculated by using Eq. (1) as reported by (Deng et al., 2015).

$$E_A = \frac{Co - Ce}{Co} x100\% \quad (1)$$

Where, Co and Ce (mg/L) are the initial concentration and final concentration at equilibrium respectively. The E_A is the removal efficiency (%).

The adsorbent capacity for the wastewater adsorption was calculated using Eq. (2):

$$Q_e = (\frac{C_o - C_e}{m})v \quad (2)$$

where; Qe is the capacity of adsorbent for the pollutant (mg/g), Co is the initial concentration of the pollutant (mg/L), Ce is the equilibrium pollutant concentration in solution (mg/L), m is the mass of adsorbent (g) and V (L) is the volume of the solution.

Characterization of Adsorbent

The FT-IR analysis for the activated-carbon groundnut pods and termite mound adsorbent was carried out before and after adsorption. 1 mg of the mixture of activated-carbon groundnut pods and termite mound was mixed with 0.5g KBr in an agate mortar and compressed at 10 tonnes cm^{-2} for 15 min under vacuum. The Fourier-transform infrared (FT-IR) analysis in the range of 700–3800 cm^{-1} was used to identify the functional groups that were responsible for adsorption using FTIR spectroscope (FT-IR-2000, Bruker) (Alade *et al.,* 2020)

The scanning electron microscopy (SEM/EDX) was performed to examine the physical structural change of samples using SEM/EDX (Phenom ProX, World Einhoven, Q150R, etherlands). The sample was placed on double-adhesive which was on a sample stub. Thereafter, it was taken to the chamber of the SEM machine where it was viewed via Navcam for focusing and little adjustment. It was then transferred to SEM mode where the focus and brightness contrasting was automatically adjusted. Afterward, the morphologies of different magnification were stored in a disk (Mohammed and Abdullah, 2018). An X-Ray Diffractometer (XRD) was employed to investigate the physical properties of the adsorbent as it relates to the crystallinity of the material. The sample was analyzed using the reflection-transmission spinner stage and the theta-theta settings. The two-theta starting position was 4θº and ends at 75 θº with a two-theta step of 0.026261 at 8.67 seconds per step. The Tube current was 40 mA and the tension was 45 VA. A programmable divergent slit was used with a 5 mm width mask and the Gonio Scan was employed (Fatimah *et al.,* 2021).

Adsorption Isotherm

The adsorption isotherm provides a relationship between the total mass of adsorbed adsorbate per unit mass of adsorbent and concentration at constant ambient conditions. In order to develop adsorption isotherms, adsorption experiments were performed. Equilibrium isotherms were determined using the optimal

parameters.

Langmuir Isotherm

The Langmuir isotherm is the simplest theoretical model for monolayer adsorption, based on the assumption that molecules are adsorbed at a fixed adsorption site and each site can hold one adsorbate molecule. It also suggests that all sites are energetically equivalent and there is no interaction between the adsorbate molecules. Langmuir isotherm is given in Eq. 3:

$$\frac{C_e}{q_e} = \frac{1}{bq_m} + \frac{C_e}{q_m} \quad (3)$$

where q_m is the maximum adsorption capacity (mg/g) and b is the Langmuir constant related to the energy of adsorption (L/mg) (Okeowo et al., 2019).

The Freundlich isotherm constants, K_f and n−1, were determined from the plot of log qe versus log Ce. Freundlich isotherm is given in Eq. 4 (Okeowo et al., 2019).

$$Log\ q_e = Log\ K_f + \frac{1}{n} Log\ Ce \quad (4)$$

Adsorption Kinetics

Sorption kinetics can be used to describe the controlling mechanism of the adsorption process. The two kinetic models, pseudo-first-order and pseudo-second-order, were used to investigate the fit experimental data from the adsorption.

Pseudo-first-order model

The adsorption kinetic data is evaluated using the pseudo-first-order equation (Lagergren's equation), which can describe the adsorption rate based on the sorption capacity of solids. The linear form of the pseudo-first-order model can be expressed as in Eq.5:

$$Log(q_e - q_t) = \log q_e - \frac{K_1}{2.303} t \quad (5)$$

where q_e and q_t are the amount of metal ion adsorbed at equilibrium and at time t (min), respectively (mg/g) and k_1 is the rate constant of pseudo-first-order adsorption (min^{-1}). (Ali et al., 2006)

Pseudo-second-order model

The adsorption kinetic may also be described by the pseudo-second-order model. The equation for linear form is shown in Eq. 6:

$$\frac{t}{qt} = \frac{1}{K_2 q_e^2} + \frac{1}{qe} t \quad (6)$$

where k_2 is the rate constant of pseudo-second-order adsorption (g/mg.min) and $K_2 q_e^2$ is the initial adsorption rate (mg/g.min) (Mustapha, et al., 2017; Aderibigbe, et al., 2020).

Results and Discussion

Characterization Studies

Heavy metals in pharmaceutical wastewater

Characterization of the pharmaceutical effluent was conducted using Atomic Adsorption Spectrophotometer (AAS) and the results were presented in Table 2. It was observed that Zinc (Zn) and Iron (Fe) appeared to be above WHO standard. The pH of the wastewater was measured and found to be 6.6.

Table 2. Results of Heavy Metals Analysis in Pharmaceutical Wastewater

Metals	WHO (2003) (mg/l)	sta Analysis result (mg/l)
Fe	0.3	0.46
Zn	0.01	0.10
Pb	0.01	0.01
Cu	0.02	0.02
Cd	0.003	ND

ND= Not Detected NS= Not Stated

Fourier transform infrared spectroscopy (FT-IR) analysis

Figure 1 shows the functional groups of the optimal adsorption with M18 in ratio (2:1) and reveals that a significant peak located around wave number 3652.8 cm^{-1} is attributed to hydroxyl groups or adsorbed water. The wide transmittance band appearing at wave number ranging from 3201.8 - 2985.6 cm^{-1} was due to C-H stretching. The absorption band observed at wavenumbers 2370.6 and 2113.4 cm^{-1} depicts a C≡C stretch. The peak at wave number 1994.1 cm^{-1} indicates C-H bending, and the bands located at wave number ranging from 1561.8 - 1524.8 cm^{-1} are ascribed to the C=C vibrations of aromatic rings. Bands appearing between wave number 1036.2 and 909.5 cm^{-1} indicate the presence of C–F stretch, acids, and phosphorous species (Kamaraj and Umamaheswari, 2019). Amole *et al.* (2020) has also obtained similar results when the FTIR characterization of $ZnCl_2$-modified groundnut shell was investigated.

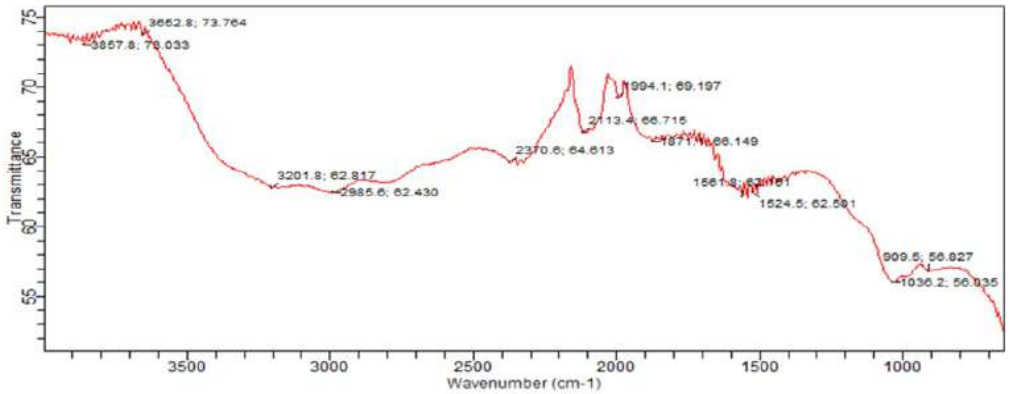

Figure 1. FT-IR Spectrum of Activated-Carbon Groundnuts Pod and Termite Mound Adsorbent

Scanning electron microscopy (SEM) analysis:

The morphological characterization of the activated-carbon groundnuts pod and termite mound adsorbent are depicted in Figure 2. The images show a rugged stone or a rocky surface. It showed that the adsorbent has a rough texture with a heterogeneous surface and a variety of randomly distributed pore sizes. There are rough potholes on top as well as crispy pits are seen. These patchy potholes are responsible for maximum adsorption of Zn(ii) and Fe(II) (Chandrasekhar *et al.,* 20

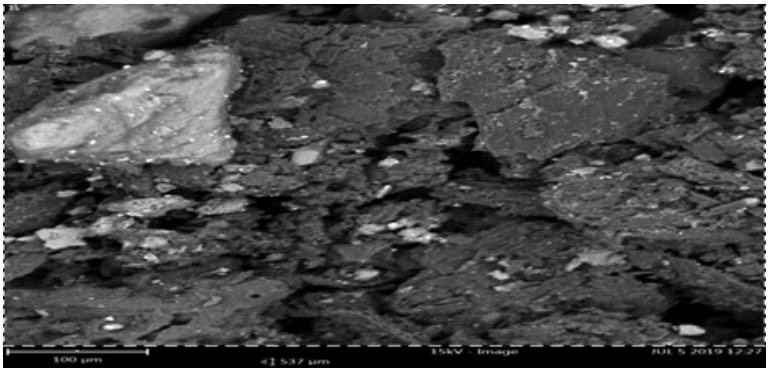

Figure 2. SEM Image of the Activated-Carbon Groundnuts Pod and Termite Mound Adsorbent.

Energy dispersive x-ray (EDX)

The elemental analyses of the activated-carbon groundnuts pod/termite mound adsorbent are depicted in Figure 3. The EDX micrograph shows the presence of Carbon, Oxygen, Silicon and Aluminium in major quantities, and of traced amounts of Titanium, Sulphur, and Chromium. This was also confirmed in Table 2. Based on these facts, it can be concluded that the prepared activated-carbonized groundnuts pod/termite mound adsorbent present has an adequate morphology for heavy metals. Similar result was also obtained by (Ajala and Ali, 2020) when groundnut shell – based activated charcoal was prepared and characterized.

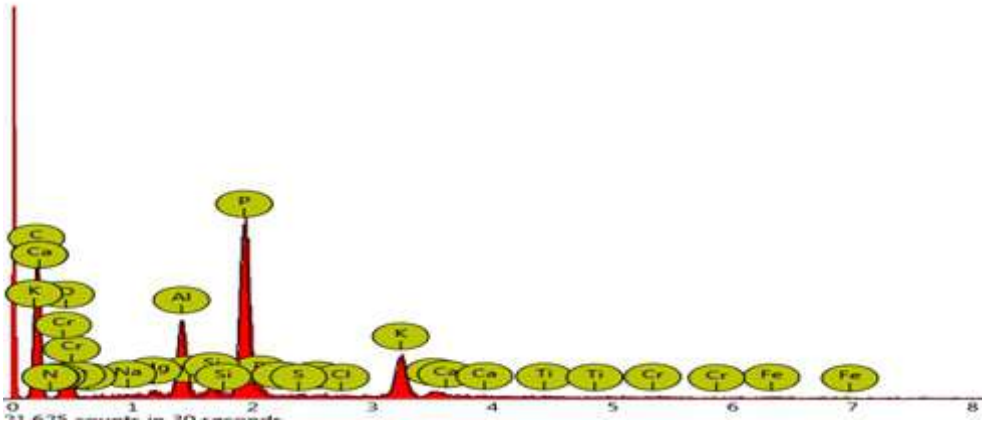

Figure 3. EDX Micrograph of the Activated-Carbon Groundnuts Pod/Termite mound Adsorbent.

Table 3. Results of Energy Dispersive X-ray (EDX) of Activated-Carbon Groundnuts Pod/Termite Mound Adsorbent.

Element Symbol	Element Name	Atomic Conc.	Weight Conc.	% Composition Element
Si	Silicon	33.74	24.38	13.72
Ta	Tantalum	4.85	22.58	12.70
P	Phosphorus	21.14	16.85	9.48
Al	Aluminium	15.87	11.02	6.21
K	Potassium	5.17	5.20	2.92
Ca	Calcium	3.05	3.15	1.77
Na	Sodium	3.40	2.01	1.13
S	Sulfur	2.31	1.91	1.07
Mg	Magnesium	2.64	1.65	0.92
C	Carbon	82.73	76.01	42.78
Fe	Iron	8.67	12.90	7.30

X-ray diffraction (XRD)

The prepared activated-carbon groundnuts pod and termite mound adsorbent was also characterized by means of X-ray diffraction. The X-ray patterns of the adsorbent are shown in Figure 4. The X-ray diffraction patterns did not exhibit well-defined peaks in any region (defined peaks related to any crystalline phase), which is an indication that no discrete mineral peaks were detected in the samples. Thus, the adsorbent had a completely amorphous structure with a noticeable hump, which signifies a high degree of disorder, typical of carbonaceous materials (Salini, , *et al.,* 2020).

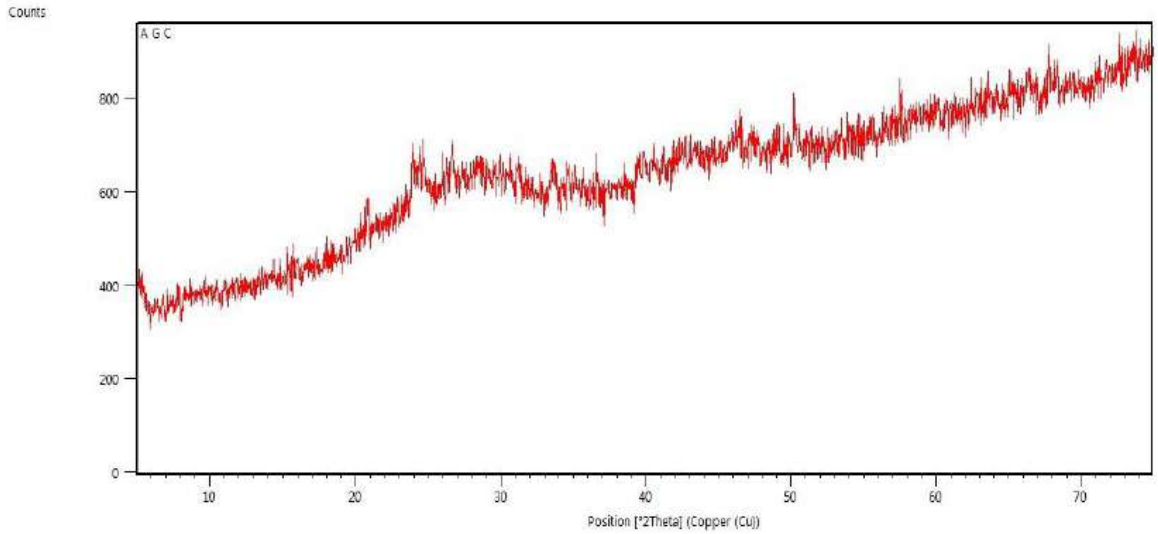

Figure 4. X-ray Diffraction of Activated-Carbonized Groundnuts Pod/Termite Mound Adsorbent.

Table 4. Effect of Ratios in Terms of Dosage at a Constant Temperature On the Removal Efficiency of Fe (II) and Zn (II) by Activated Carbonized Groundnuts Pod /Termite Mound Adsorbent.

Ratios	Co (mg/l)	Ce (mg/l)	Removal Efficiency% Fe	Co (mg/l)	Ce (mg/l)	Removal Efficiency% Zn^{2+}
M1	0.46	0.08	82.60	0.10	0.22	0.00
M2	0.46	0.08	82.60	0.10	0.08	2.00
M3	0.46	0.05	89.13	0.10	0.15	0.00
M4	0.46	0.07	84.78	0.10	0.60	0.00
M5	0.46	0.06	86.96	0.10	0.60	0.00
M6	0.46	0.06	86.96	0.10	0.40	0.00
M7	0.46	0.07	84.78	0.10	0.18	0.00
M8	0.46	0.07	84.78	0.10	0.99	0.00
M9	0.46	0.07	84.78	0.10	0.40	0.00
M10	0.46	0.05	89.13	0.10	0.10	0.00
M11	0.46	0.05	89.13	0.10	0.10	0.00
M12	0.46	0.06	86.96	0.10	0.14	0.00
M13	0.46	0.25	45.65	0.10	0.43	0.00
M14	0.46	0.04	91.30	0.10	0.05	50.00
M15	0.46	0.04	91.30	0.10	0.08	2.00
M16	0.46	0.06	86.96	0.10	0.09	10.00
M17	0.46	0.07	84.86	0.10	0.20	0.00
M18	0.46	0.04	91.30	0.10	0.05	50.00
M19	0.46	0.06	86.96	0.10	0.30	0.00
M20	0.46	0.07	84.86	0.10	0.90	0.00
M21	0.46	0.08	82.60	0.10	0.30	0.00
M22	0.46	0.08	82.60	0.10	0.42	0.00
M23	0.46	0.06	86.96	0.10	0.50	0.00
M24	0.46	0.10	78.26	0.10	0.50	0.00
M25	0.46	0.07	84.86	0.10	0.84	0.00
M26	0.46	0.05	89.13	0.10	0.30	0.00
M27	0.46	0.06	86.96	0.10	0.42	0.00

Optimization Studies

The design of the optimization experiment (DOE) is presented in Table 5. It was observed that the optimal factors for Fe (II) removed by activated carbonized groundnuts pod and termite mound is 90 mins, 0.1 g/l dosages and temperature of 25 °C. The optimum removal efficiency for Fe (II) was higher. The removal efficiency was excellent for Fe (II), this implies that groundnuts pod and termite mound are excellent adsorbents for the removal of Fe (II) from polluted effluent. The adsorption of Zn (II) didn't occur, this might be as a result of the high percentage of Zn (II) in the termite mound, and hence given selective adsorption and rendering the termite mound unsuitable for the removal of Zn (II).

Table 5. Box-Behnken Design of Optimization Experiments.

	Factor			Response	
Run	Temperature	Dosage	Time	Removal Efficiency (Fe^{2+})	Removal Efficiency (Zn^{2+})
	°C	g/l	Min	%	%
1	35	0.15	90	91.3	0.00
2	35	0.1	60	95.7	0.00
3	35	0.05	90	84.8	0.00
4	35	0.15	30	91.3	0.00
5	35	0.1	60	89.1	0.00
6	45	0.1	90	82.6	0.00
7	45	0.1	30	89.1	0.00
8	35	0.1	60	89.1	0.00
9	35	0.1	60	93.5	0.00
10	45	0.15	60	95.7	0.00
11	25	0.05	60	93.5	0.00
12	35	0.1	60	91.3	0.00
13	25	0.1	30	89.1	0.00
14	25	0.15	60	91.3	0.00
15	25	0.1	90	95.72	0.00
16	35	0.05	30	91.3	0.00
17	45	0.05	60	93.5	0.00

Effect of process parameters on Fe(II) adsorption

The middle thick line is the line of interest in all one-factor plots presented from Design expert 10.0.1. Figure 5, shows the effect of temperature on the adsorption of Fe(II). A decrease was observed with an increase in temperature, however, at the maximum of about 25 °C, a drop in adsorption was noticed from careful observation of the y-axis. It can be opined that the effect of temperature on the process is only marginal. This is a key pointer towards a physical adsorption process where the effect of temperature is less pronounced and lower temperature tends to reduce the amount adsorbed. Figure 6 shows the effect of adsorbent dosage on the adsorption of Fe(II). The amount of Fe(II) adsorbed increases with increasing dosage. This is expected as a higher dosage indicates the greater number of active sites available for adsorption. The trend was observed over the entire range of the factor studied. Figure 7 shows the effect of time on the adsorption of Fe(II) and can be observed that the amount adsorbed increases steadily as time fluctuates. Hence, the maximum adsorption is observed at 90 min.

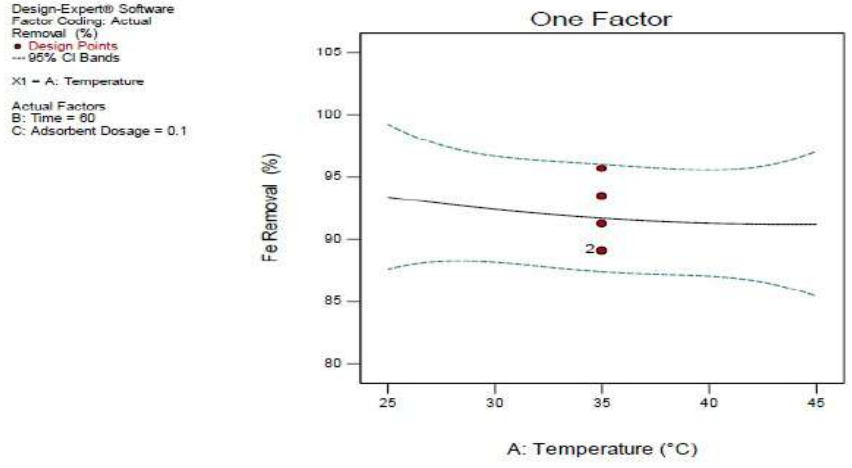

Figure 5. Effect of Temperature on Fe(II) Adsorption.

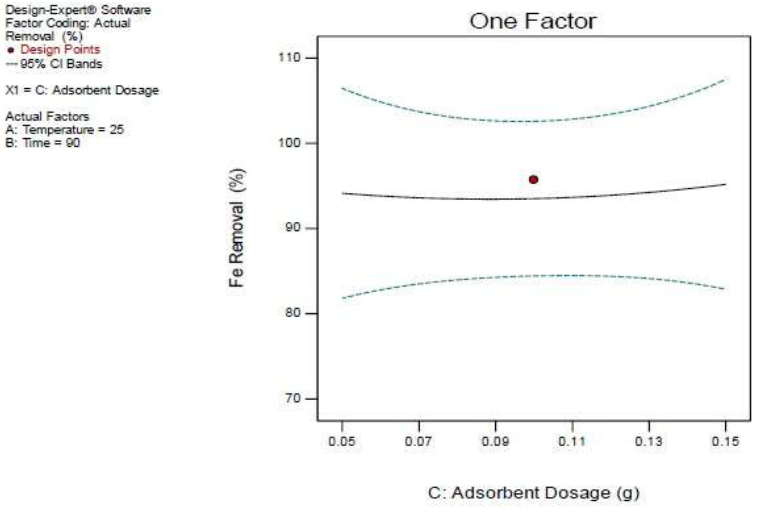

Figure 6. Effect of Adsorbent Dosage on Fe (II) Adsorption.

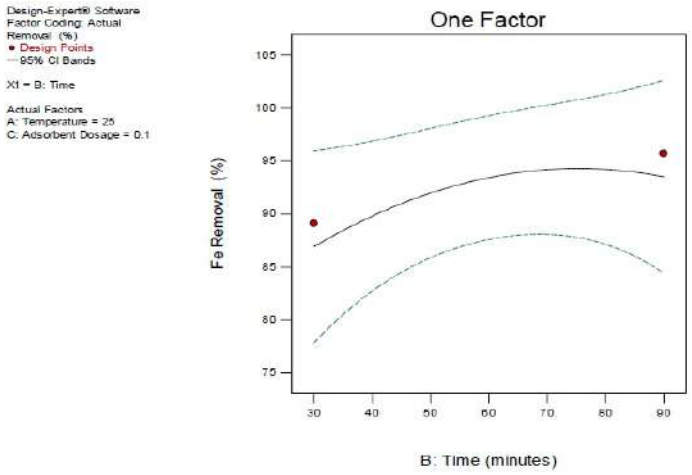

Figure 7. Effect of Time on Fe(II) Adsorption

Adsorption equilibrium etudies

The result of the equilibrium experiment for Fe(II) result was computed and fitted into the equilibrium isotherm as shown in Figure 8. The result was fitted to the Langmuir isotherm. The coefficient of determination (R^2) indicates to what extent the variability of the data is captured by the model. The R-squared values of the plots reveal that the Langmuir isotherm (R^2= 0.9997) fit for the adsorption of Fe (II) unto the groundnut pods and termite mound absorbent. The maximum adsorption capacity q_m was obtained as 0.3897 mg/g while the Langmuir constant (b) related to the energy affinity or interaction between the adsorbate and adsorbent was obtained as 371.895 L/mg. Also, the R_L was found to be a positive value of 0.0088, indicating the feasibility of adsorption process (Okeowo et al., 2019). The Freundlich isotherm revealed a R^2 value of 0.9765. The Freundlich isotherm revealed a R^2 value of 0.9765. The K_f and n value were found to be 0.317 and -11.5 respectively. This value of K_f indicates that a low adsorption intensity while the negative value of n indicates a poor adsorption process, which mean that the Freundlich isotherm does not fit the adsorption process (Okeowo *et al.*, 2019).

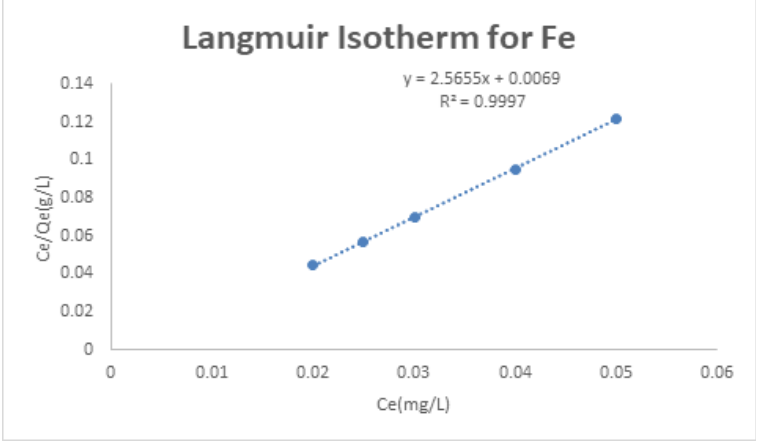

Figure 8. Langmuir Isotherm Plot for Fe (II) Adsorption

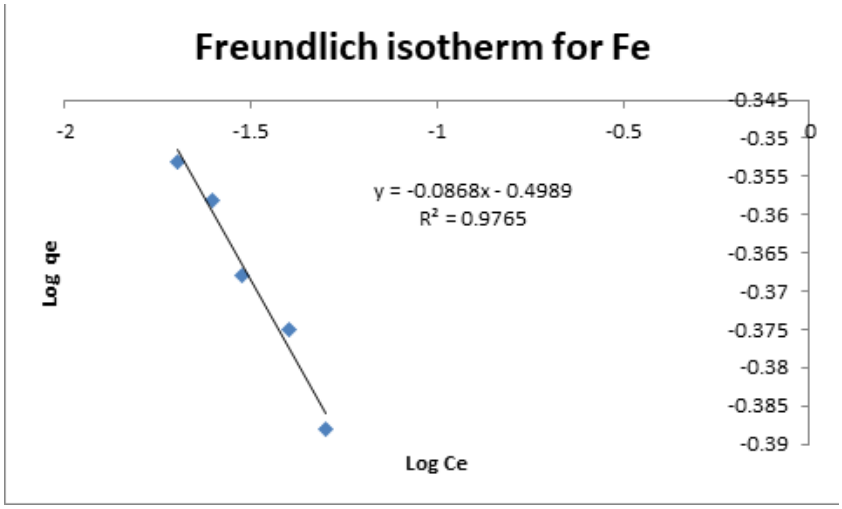

Figure 9. Freundlich isotherm Plot for Fe (II) Adsorption

Adsorption kinetics studies

These results were computed and fitted into the various kinetic models. Fe(II) adsorption result was fitted to the pseudo-first order and pseudo-second order models. The plots of the different kinetic models for Fe(II) adsorption are shown in Figures 10 and Figure 11. From R^2 values, it can be stated that the model of best fit is pseudo-first order model (R^2 = 1). For pseudo-first order (K_1) and pseudo-second order (K_2) rate constant were found to be 0.000161 min^{-1} and 5.0353 g/mg.min respectively (Alade *et al.,* 2020). Furthermore, the experimental equilibrium adsorption capacity for Fe(ii) was found to be 0.465mg/g. This is in much agreement with the calculated equilibrium adsorption capacity obtained from the pseudo-first order kinetics (0.44mg/g). Hence, confirms the fitting of the adsorption process to the pseudo first order kinetics (Gupta and Abdul Rafe, 2013)

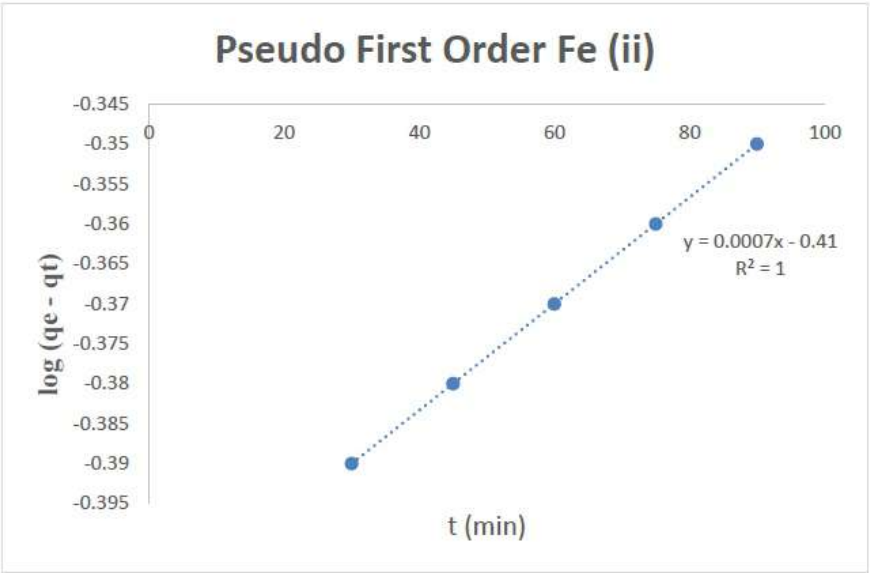

Figure 10. Pseudo-First Order Plot for Fe (II) Adsorption.

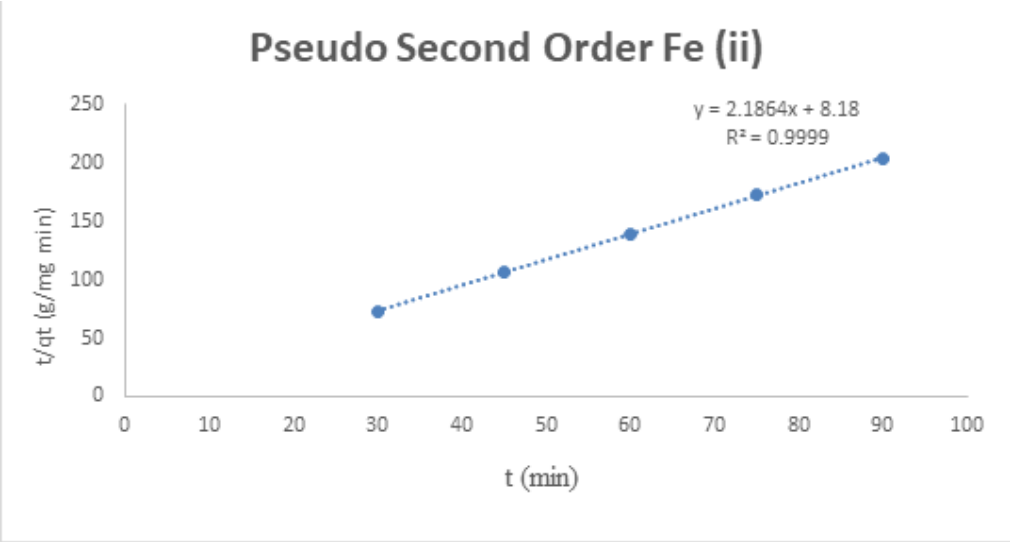

Figure 11. Pseudo-Second Order Plot for Fe (ii) Adsorption.

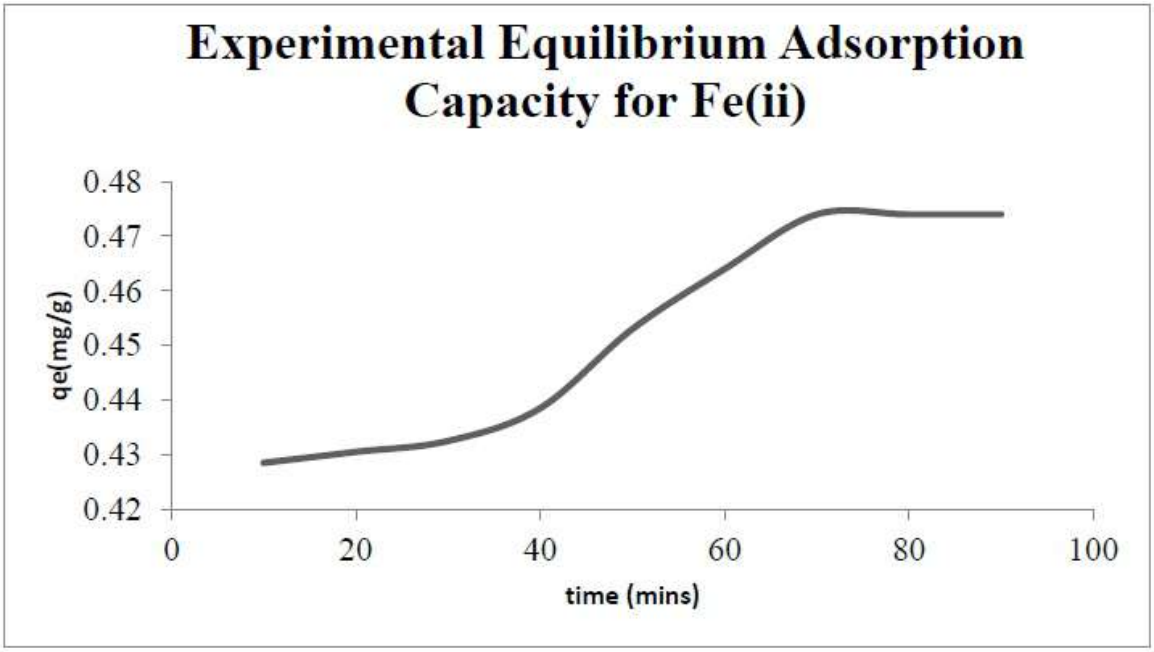

Figure 12. The Experimental Equilibrium Adsorption Capacity for Fe (ii)

Table 7. Summary of Kinetic Model Result for Fe(II) Adsorption.

Metal	C_o (mg/L)	Pseudo -first order			Pseudo -second order		
Fe (II)	0.46	K_1 (min $^{-1}$)	q_{cal} (mg/g)	R^2	K_2 (g/mg .min)	q_{cal} (mg/g)	R^2
		0.000161	0.44 9	1.000	5.0353	0.424	0.9999

Conclusion

This study showed that the activated-carbonized groundnuts pod and termite mound adsorbent has the potential to effectively remove Fe^{2+} from aqueous solutions and can be used as a substitute for commercially expensive adsorbents. In furtherance to this, the optimal Fe^{2+} removal of 95.72 % was achieved at optimal parameters of 25 °C, 90 mins and 0.1 g adsorbent loading. The Langmuir isotherm based on its correlation coefficient value (R^2= 0.9997 fits the model than the Freundlich isotherm. Also, the kinetic data agrees well with the pseudo-first-order model (R^2= 1.000) which was more fitting to the adsorption data obtained for the Fe^{2+}. The experimental equilibrium adsorption capacity q_{exp} of 0.465 mg/g (Fe(ii)) also agrees well with the pseudo first order having the calculated equilibrium adsorption capacity to be 0.44 mg/g.

References

Aderibigbe, F. A., Mohammed, I. A., Mustapha, S.I., Saka, H.B., Amosa, M. K., Adejumo, A. L., Owolabi, R. and Shittu A.B. (2020). Removal of Cod from Pharmaceutical Wastewater Using Sugarcane Bagasse and Bentonite Clay. *LAUTECH J. Eng Technol* 14 (1) 2020:107-115.

Aderibigbe, F. A., Mohammed, I. A., Mustapha, S.I., Saka, H.B., Amosa, M. K., Adejumo, A. L., Owolabi, R.U. and Moshood, A.O. (2021). Removal Of Phenol from Pharmaceutical Effluents Using Locust Bean Pod and Bentonite Clay. *LAUTECH J. Eng Technol* 15 (1) 2021: 117-124

Ajala, L.O and Ali, E.E. (2020). Preparation and characterization of groundnut shell-based activated charcoal. *Journal of applied science and environmental Management, 24,* (12),2139-2146

Alade, A.O., Arinkoola, A.O, Afolabi, T.J., Adegbola, A.A., Oloyede, O.G., Odiase, P.O. (2020). D-Optimal Optimization of Microwaveassisted Synthesis of Moringa Oleifera Pod Activated Carbon and Application to Methylene Blue Adsorption. *Annals Faculty of Engineering Hunedoara- International Journal of Engineering,* 189- 203

Ali, R., Rao, K., and Kashifuddin, M. (2014). Kinetics and isotherm studies of Cd (II) adsorption from aqueous solution utilizing seeds of bottlebrush plant (Callistemon chisholmii). *Appl Water Sci J.,* 4: 371-383. https://doi.org/10.1007/s13201-014-0153-2

Amole, A.R., Araromi, D.O., Alade, A.O., Afolabi, T.J., Adeyi, V.A (2020). Biosorptive removal of nitrophenol from aqueous solution using $ZnCl_2$-modified groundnut shell: optimization, equilibrium, kinetic, and thermodynamic studies. *Int. J. Environ. Sci. Technol.* (2020). https://doi.org/10.1007/s13762-020-02939-y

Cabriga, C.K., Clarete, K.V.B., Zhang, J.A., Pacia, R.M., Ko, Y.S and Castro, J.C. (2021). Evaluation of biochar derived from the slow pyrolysis of rice straw as a potential adsorbent for carbon dioxide. *Biomass conversion and biorefinery*, 1-8

Chandrasekhar, S.P., Gunjal, D.B., Naik, V.M., Harale, S.N., Jagadale, S.D., Kadam, A.N., Partil, P.S., Kolekar, G.B. and Gore, A.H. (2019). Waste tea residue as a low cost adsorbent for removal of hydralazine hydrochloride pharmaceutical pollutant aqueous media: an environment remediation. Journal of cleaner production, *206*,

407-418

Chen, W., He, Z., Huang, G., Wu, C., Chen, W., and Liu, X. (2018). Direct Z-Scheme 2D/2D $MnIn_2$ S_4/g-C_3N_4 architectures with highly efficient photocatalytic activities towards treatment of pharmaceutical wastewater and hydrogen evolution. *Chemical Eng J.* 359: 244-253. https://doi.org/10.1016/j.cej.2018.11.141

Deng, S., Hu, B., Chen, T., Huang, J., and Wang, Y. (2015). Activated carbons prepared from peanut shell and sunflower seed shell for high CO_2 adsorption. *J. inter Adsoprtion*, Springer. 21: 125-133. https://doi.org/10.1007/s10450-015-9655-y

Farombi, A.G. (2020). Adsorption of phenol from waste water Using Microwave assisted Ag-Au Nanoparticle – Modified Mango Seed Shell-Activated Carbon. *International Journal of Environmental Research,* 1-19

Fatimah, S., Ragadhita, R., Al-Husaeni, D. F. and Nanadiyanto, A.B.D. (2022). How to calculate crystalline size from X-ray diffraction (XRD) using Scherrer Method. *ASEAN Journal of Science and Engineering, 2,* (1), 65-76

Fufa, F., and Engineering, E. (2016). Experimental Evaluation of Activated Termite Mound for Fluoride Adsorption. *IOSR J. Environmental Sci. Toxicology Food Technol.*, 10(8): 119–132. https://doi.org/10.9790/2402-100802119132

Gisi, S.D., Lofrano, G., Grassi, M and Notarnicola, M (2016). Characteristics and adsorption capacities of low-cost sorbents for waste water treatment: A review. Sustainable Materials and Technologies, *9*, 10-40.

Gupta A, Abdu Rafe M (2013) Removal of phenol from wastewater using mango peel. *International Journal of Engineering and Technology* Res 1:58–62

Gupta, V. K., and Ali, I. (2004). Removal of lead and chromium from wastewater using bagasse fly ash — a sugar industry waste. *J. Colloid Interface Sci.*, 271:321–328. https://doi.org/10.1016/j.jcis.2003.11.007

Gupta, V. K., Carrott, P. J. M., and Carrott, M. M. L. R. (2009). Low-Cost Adsorbents : Growing Approach to Wastewater Treatment — a Review. *Critical Reviews in Environmental Sci. Tech. J.*, 39(10): 783–842. https://doi.org/10.1080/10643380801977610

Habeeb, O. A., Yasin, F., and Danhassan, U. A. (2014). Characterization and application of chicken eggshell as green adsorbents for removal of H_2S from wastewaters. *IOSR J. Environmental Sci. Toxicology Food Technol.*, 8(11): 7–12

Kamaraj, M. and Umamaheswari, P. (2017). Preparation and characterization of Groundnut shell activated carbon as an efficient adsorbent for the removal of Methylene blue dye from aqueous solution with microbiostatic activity. *J. Mat. Environmental Sci.,* 8(6): 2019–2025.

Larous, S. and, Meniai, A-h . (2012). The use of sawdust as by-product adsorbent of organic pollutant from wastewater : adsorption of phenol. Sciverse Energy Direct, *Energy Procedia J.* Elsevier, 18: 905–914. https://doi.org/10.1016/j.egypro.20

12.05.105

Larsson, M., Nosrati, A., Kaur, S., Wagner, J., Baus, U., Nyden, M (2018). Copper removal from acid mine drainage – polluted water using glutaraldehyde-polyethyleneimine modified diatomaceous earth particles. *Heliyon*, *4,* (2). doi.org/10.101016/j.heliyon.2018.e00520.

Mohamed, N. R (2013). Adsorption technique for the removal of organic pollutants from water and waste water. Doi:10.5772/54048

Mohammed, A. and Abdullah, A. (2018). Scanning Electron microscopy (SEM): A review. *Proceedings of the 2018 international conference on hydraulics and pneumatics HERVEX, Baile Govora, Romania*, 7-9.

Mustapha, S. I., Adewoye, L. T., Aderibigbe, F. A., Alhaji, M. H., Adekola, M. I. and Tijani, I. A. (2017). Removal of Lead and Chromium from Aqueous Solution onto Flamboyant (*Delonix regia*) Pod Activated Carbon. *Nigerian J. Technol Dev, Vol.* 14, No. 2, 56-66

Okeowo, I.O., Balogun, E.O., Ademola, A.J., Alade, A.O., Afolabi, T.J., Dada, E.O.,

Salini, .N.G., Ismayii, K.M M. and Antony, R. (2020). Mesoporous Carbonaceous Material from Expand Polystyrene and Bentonite for instantaneous Degradation of mixture of Dyes. 1-29Doi.org/10.21203/rs-589419/v1

Stylianou, M. A., Inglezakis, V. J., Moustakas, K. G., Malamis, S. P., and Loizidou, M. D. (2007). Removal of Cu (II) in fixed bed and batch reactors using natural zeolite and exfoliated vermiculite as adsorbents. *J. of Desalination.*, 215:133–142. https://doi.org/10.1016/j.desal.2006.10.031

Trivedi N.S., and Mandavgane S.A. (2016) Utilization of an Agro Waste, Groundnut Shell Ash, for Removal of 2,4-Dichlorophenoxyacetic Acid. In: Regupathi I., Shetty K V., Thanabalan M. (eds) *Recent Advances in Chemical Engineering*. Springer, Singapore. https://doi.org/10.1007/978-981-10-1633-2_18

Trivedi, N. S., Kharkar, R. A., and Mandavgane, S. A. (2016). 2, 4-Dichlorophenoxyacetic acid adsorption on adsorbent prepared from groundnut shell : Effect of preparation conditions on equilibrium adsorption capacity. *Arabian J. Chem.*, 12(8):4541-4549. https://doi.org/10.1016/j.arabjc.2016.07.022